narra j

Short Communication

Therapeutic potential of thymoquinone in regulating p63, claudin, and periostin in chronic rhinosinusitis with nasal polyps: An animal model study

Loriana Ulfa[1,2*], Delfitri Munir[3], Andrina YM. Rambe[3], Farhat Farhat[3], Retno S. Wardani[4,5], Mustafa M. Amin[1,6], Devira Zahara[3] and Dedi Ardinata[7]

[1]Philosophy Doctor in Medicine Program, Faculty of Medicine, Universitas Sumatera Utara, Medan, Indonesia; [2]Department of Ear, Nose, and Throat, Faculty of Medicine, Universitas Riau, Pekanbaru, Indonesia; [3]Department of Ear, Nose, and Throat, Faculty of Medicine, Universitas Sumatera Utara, Medan, Indonesia; [4]Department of Ear, Nose, and Throat, Faculty of Medicine, Universitas Indonesia, Jakarta, Indonesia; [5]Department of Ear, Nose, and Throat, Dr. Cipto Mangunkusumo Hospital, Jakarta, Indonesia; [6]Department of Psychiatry, Faculty of Medicine, Universitas Sumatera Utara, Medan, Indonesia; [7]Faculty of Medicine, Universitas Sumatera Utara, Medan, Indonesia

*Corresponding author: zoelfa_dr@yahoo.co.id

Abstract

High recurrence rate and the necessity for repeated surgical interventions contribute to the chronicity and treatment-resistant nature of chronic rhinosinusitis with nasal polyps (CRSwNP). Thymoquinone, known for its protective effects on epithelial integrity, has not been previously explored in CRSwNP. The aim of this study was to investigate the therapeutic potential of thymoquinone to restore epithelial integrity by assessing p63 transcription factor and claudin protein expressions, as well as periostin mRNA expression in an animal model. An in vivo study using post-test-only control group design was conducted in which male Wistar rats were randomly assigned to three groups, each consisting of 10 animals: healthy group, CRSwNP group, and thymoquinone-treated group for three weeks. Immunohistochemistry was used to analyze the p63 and claudin protein expressions, while periostin mRNA expression was quantified using quantitative reverse transcription polymerase chain reaction (qRT-PCR). This study found that thymoquinone significantly reduced p63 transcription factor expression compared to the untreated CRSwNP group (p=0.009). Claudin protein expression was significantly higher in thymoquinone-treated group compared to CRSwNP group (p=0.007), indicating improved epithelial barrier function. Periostin mRNA expression showed no significant difference between healthy and thymoquinone-treated groups (p=0.564), but a significant decrease was observed in CRSwNP group compared to thymoquinone-treated group (p=0.000) and between the healthy and CRSwNP groups (p=0.002), suggesting attenuation of tissue remodeling and inflammation. In conclusion, thymoquinone could enhance sinonasal epithelial barrier integrity in CRSwNP by downregulating p63 transcription factor, upregulating claudin protein expression, and reducing periostin mRNA expression. These findings emphasize the potential of thymoquinone as a therapeutic agent to mitigate inflammation and tissue remodeling in CRSwNP, warranting further investigation as a novel treatment option.

Keywords: CRSwNP, thymoquinone, p63 transcription factor, claudin, periostin

Introduction

Chronic rhinosinusitis with nasal polyp (CRSwNP) is a chronic inflammatory disorder of the sinonasal mucosa, characterized by recurrent polyps and symptoms such as nasal obstruction,

https://narraj.org/

Received: November 1, 2024 - Accepted: February 13, 2025 - Published online: March 16, 2025

anosmia, and postnasal drip [1]. CRSwNP accounts for 25–30% of chronic rhinosinusitis (CRS) cases, affecting 1–4% of the population, with an average patient age of 42 years [2]. The recurrence rate of CRSwNP following surgery is reported to be 78.9% over 12 years, with 36.8% requiring additional surgical interventions [3]. The high recurrence rate and need for repeated surgical interventions in CRSwNP highlighted its chronic and refractory nature, emphasizing the importance of early risk factor identification and personalized treatment strategies.

Recent studies have suggested that defects in the physical barrier of the epithelium play an important role in the pathogenesis of CRSwNP [4-6]. One of the main structures forming the physical barrier to maintain the integrity of the nasal epithelium is the tight junction [4]. Tight junctions function to regulate epithelial permeability, prevent the entry of foreign substances from outside the body and increase the integrity of the mechanical epithelium [7,8]. The integrity of the epithelial barrier in CRS is disrupted resulting in a chronic nasal inflammatory process that leads to the development of CRSwNP [5,9]. Tight junctions contain several transmembrane proteins, such as occludin and claudin which are targets of the *p63* gene that plays a role in modulating the function of the physical barrier of the epithelium in cases of CRS [10,11]. In addition to epithelial barrier damage, CRSwNP can also be caused by *Staphylococcus aureus* enterotoxin B (SEB) [12]. A recent study reported that SEB nasal colonization was detected in 67% of CRSwNP patients [12]. Destruction of epithelial barrier integrity has been reported as the main pathogenic mechanism associated with SEB in CRSwNP [12].

Epithelial barrier disruption allows pollutants and allergens to penetrate the subepithelial layer, triggering and exacerbating inflammation, which is associated with reduced claudin expression [13,14]. The *p63* gene regulates the epithelial barrier by promoting the expression of tight junction proteins and ciliogenesis in the sinonasal epithelium [15]. In CRS, epithelial and basement membrane damage initiates polyp formation through epithelial-to-mesenchymal transition (EMT), a process characterized by epithelial cell differentiation and functional transformation into mesenchymal cells [5]. EMT leads to increased extracellular matrix protein production, including periostin, which is significantly elevated in CRSwNP and serves as a biomarker for this condition [5].

Thymoquinone, an active compound with diverse biological properties, has been shown to enhance epithelial barrier function [16,17]. A previous study demonstrated that administration of thymoquinone in Wistar rats exposed to acrylamide increased occludin expression by 99% in testicular tissue, restoring tight junction integrity [18]. The reduction in tight junction protein expression is mediated by elevated p63 transcription factor levels, suggesting that improved tight junction integrity correlates with decreased p63 expression and increased claudin levels [19]. Currently, to the best of our knowledge, no studies have explored the effects of thymoquinone on periostin mRNA expression or its role in inhibiting the EMT process in CRSwNP [20]. Additionally, the effect of thymoquinone on p63 and claudin expression in CRSwNP remains unexplored. While omalizumab has demonstrated efficacy in reducing periostin mRNA expression in CRSwNP, its high cost limits accessibility [21], necessitating research into alternative therapies such as thymoquinone.

Thymoquinone has shown effectiveness in improving epithelial integrity in rat testicular tissue and was administered at a dose of 10 mg/kg/day, which has previously demonstrated efficacy in Wistar rats over eight weeks [3,18,21]; however, its effects on CRSwNP have not been investigated. Preclinical animal studies are crucial for evaluating drug dosages and potential side effects in initial therapeutic investigations. The aim of this study was to investigate whether thymoquinone could restore epithelial integrity by assessing its potential to modulate p63 transcription factor, claudin expression, and periostin mRNA expression in Wistar rat models. This investigation aimed to evaluate both the extent of modulation and directionality changes in these biomarkers, providing insight into thymoquinone's therapeutic potential for epithelial repair. Wistar rats were selected as the experimental model due to the anatomical similarity of the squamous epithelium-lined nasal cavity to humans, despite the absence of nasal hair follicles in rats, as the nasal cavity primarily serves olfactory functions [22].

Methods

Study design and setting

An in vivo study using a post-test-only experimental design was conducted at the Laboratory of Stem Cell and Cancer Research, Semarang, Central Java, Indonesia, from December 2023 to May 2024. Male Wistar rats (*Rattus norvegicus*), weighing 180–200 g, were used to create the CRSwNP animal model and were allocated into three groups: healthy group, untreated CRSwNP group, and thymoquinone-treated CRSwNP group. Immunohistochemistry (IHC) analysis was used to analyze p63 and claudin protein expression, while periostin mRNA expression was quantified using quantitative reverse transcription polymerase chain reaction (qRT-PCR).

Sample size, eligibility criteria, and randomization

Inclusion criteria were male Wistar rats (*Rattus norvegicus*) aged six weeks, weighing between 180–200 g, and in good health, as confirmed by a veterinary examination. Rats with pre-existing conditions, respiratory or systemic abnormalities, or abnormal behavior were excluded. Rats that did not survive during the study period were considered dropouts. The sample size was determined using the Federer formula for experimental design, ensuring a minimum degree of freedom error of 15. This calculation resulted in a total of 30 rats, with 10 rats per group across three groups. Neither the researchers nor the veterinarian was blinded during the study. Simple randomization, using a randomization table, was employed to assign rats to each group purely by chance, reducing the risk of confounding variables affecting the results. Daily evaluations monitored behavior, activity, respiratory function, injuries, and body weight. One rat from each group was terminated for CRSwNP confirmation after three weeks of intervention.

Animal preparation

All rats were housed in standard laboratory cages with free access to standard chow and water throughout the study period. Environmental conditions were carefully regulated, maintaining a temperature of 26°C, relative humidity between 50–60%, and a 12-hour light/dark cycle to ensure consistency. Prior to experimental procedures, the rats underwent a one-week acclimatization period to minimize potential stress and ensure adaptation to laboratory conditions.

Thymoquinone solution preparation

Pure crystalline thymoquinone ($C_{10}H_{12}O_2$) (Sigma Aldrich, St. Louis, Missouri, USA) was used in this study. The thymoquinone solution was prepared by dissolving the crystalline compound in 1% dimethyl sulfoxide (DMSO) (Sigma Aldrich, St. Louis, Missouri, USA), which was selected for its high solubility and precise measurability. A dose of 10 mg/kg body weight (BW) thymoquinone was administered intranasally to the thymoquinone-treated groups. The solubility of thymoquinone in DMSO is 14 mg/mL [18].

Intervention

Rats were randomly assigned to three groups, each consisting of 10 animals: the healthy group, the CRSwNP group, and the thymoquinone-treated CRSwNP group. Rats were systemically sensitized on days 0 and 7 with intraperitoneal injections of phosphate-buffered saline (PBS) (Gibco, Massachusetts, USA) for the healthy mice group. For the CRSwNP and thymoquinone-treated groups (20 rats in total), each rat received an injection of 25 mg of ovalbumin (OVA) grade V (Sigma Aldrich, St. Louis, Missouri, USA) combined with 2 mg of aluminum hydroxide gel (Sigma Aldrich, St. Louis, Missouri, USA) to induce an allergic inflammatory response. Following systemic sensitization, rats underwent daily intranasal challenges with either PBS or 6% OVA from days 14 to 20; the healthy group received PBS nasal challenges, while the CRSwNP and thymoquinone-treated groups were challenged with 6% OVA three times per week for two weeks. One representative rat from each group was euthanized for histopathological evaluation to confirm CRSwNP-like tissue. The nasal epithelial lining exhibited structural variations, ranging from simple to multilayered columnar cells with intact ciliation. Additionally, a prominently thickened basement membrane further confirmed the successful induction of CRSwNP. On day 35, both the CRSwNP and thymoquinone-treated groups received 6% OVA and *Staphylococcus*

aureus enterotoxin B (SEB; 10 ng) intranasally three times per week for eight weeks, while the thymoquinone-treated group was additionally treated with a thymoquinone solution (Sigma Aldrich, Missouri, USA) at a dose of 10 mg/kg BW daily for eight weeks (**Figure 1**).

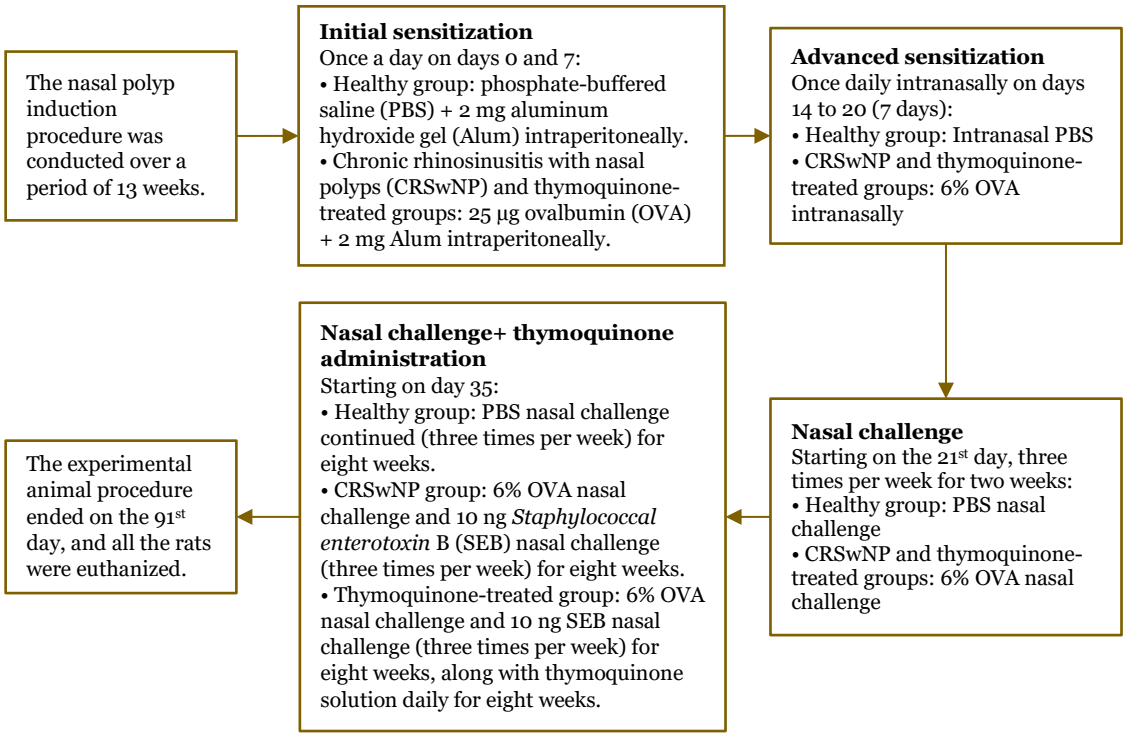

Figure 1. Study flow of the present study, describing the timeline of initial sensitization, advanced sensitization, nasal challenges, and thymoquinone treatment across the different groups.

Nasal cavity tissue sample collection

Intravascular perfusion was conducted using 200 mL of 2% paraformaldehyde in 0.1 M PBS to fix tissues. For nasal cavity sample preparation, rats were decapitated, and the heads were immobilized. The lower jaw and tongue were dissected, and the snout was severed using a number 22 scalpel with a transverse incision positioned behind the posterior molars, following the alignment of the hard palate. After removing the skin and soft tissue, the external nares were flushed with PBS to eliminate blood within the nasal cavity [23]. Nasal cavity mucosal samples were immediately fixed in 10% buffered formalin for histopathological analysis or RNA later for qPCR. Specimens were decalcified in 0.25 M ethylenediaminetetraacetic acid (EDTA) dissolved in PBS until sufficient softening was attained. Histopathological processing, carried out at the Laboratory of Animal Health, Semarang, Central Java, Indonesia, included sequential dehydration in graded ethyl alcohol, clearing in xylene, and embedding in paraffin at 60°C. The samples were sectioned into 4 µm slices using a microtome, stained with hematoxylin and eosin (HE), and analyzed under a light microscope [24].

Immunohistochemistry analysis

Tissue preparation for slide analysis involved attaching samples to poly-L-lysine-coated slides, followed by heating at 60°C. The slides were deparaffinized with xylene and rehydrated through graded ethanol solutions. Antigen retrieval was performed by incubating the slides in citrate buffer (pH 6.5) at 90°C for 30 minutes, followed by cooling to room temperature and rinsing with PBS. Endogenous peroxidase activity was blocked using hydrogen peroxide (H_2O_2), and non-specific background staining was reduced with a background blocker. The slides were incubated with primary antibodies (p63 and claudin) and secondary antibodies, with the Trekkie Universal Link Secondary Antibody (Starr Trek Universal-HRP Detection Kit, Biocare Medical, California, USA) applied for 60 minutes for the primary antibody and 45 minutes for the secondary antibody. Antigen-antibody complexes were visualized using 3,3'-Diaminobenzidine (DAB) chromogen and counterstained with Mayer's hematoxylin for three minutes. The slides were dehydrated through

graded ethanol, cleared with xylene, and mounted with Entellan (Sigma Aldrich, St. Louis, Missouri, USA). Staining results were assessed using a semi-quantitative scoring system: 0 (no staining), 1+ (weak intensity), 2+ (moderate intensity), and 3+ (strong intensity) [25]. Scoring was based on observations from five fields of view per slide at 200× magnification, with assessments conducted in representative areas.

RNA extraction

RNA extraction from nasal cavity tissue samples was performed using TRIzol reagent (Invitrogen, Massachusetts, USA) according to the manufacturer's instructions. Approximately 50 mg of tissue was placed directly in 1 mL of TRIzol reagent for RNA isolation. After incubation, 200 µL of chloroform was added, and the mixture was shaken vigorously for 15 seconds. The sample was then centrifuged at 20,000×g for 15 minutes at 4°C, and the clear upper aqueous phase containing the RNA was carefully transferred into a fresh 1.5 mL tube. Isopropanol (0.5 mL per 1 mL of TRIzol) was added, mixed by gentle inversion, and incubated at room temperature for 10 minutes. The sample was centrifuged again at 20,000×g for 15 minutes at 4°C, and the supernatant was discarded. The RNA pellet was washed with 1 mL of 75% ethanol and centrifuged at 15,000×g for 5 minutes at 4°C. After removing excess ethanol, the RNA pellet was dissolved in 100 µL of nuclease-free water (Invitrogen, Massachusetts, USA). RNA concentration and purity were evaluated using a NanoDrop spectrophotometer (Thermo Fisher Scientific, Massachusetts, USA), with absorbance ratios measured at 260/280 nm and 260/230 nm to assess sample quality.

Quantitative reverse transcription polymerase chain reaction (qRT-PCR)

First-strand cDNA synthesis was performed using 1 µg of total RNA and SuperScript II reverse transcriptase (Invitrogen, Massachusetts, USA) following the manufacturer's instructions. The reverse transcription reaction utilized an oligo d[T] primer, with an initial incubation at 70°C for 10 minutes to denature RNA secondary structures, followed by 30 minutes at 45°C for cDNA synthesis. qRT-PCR was conducted using a PCRmax Eco 48 system (Illumina, San Diego, California, USA) with a 20 µL reaction volume. The qPCR mixture comprised 10 µL of SYBR Green Master Mix (KAPA Biosystems, Sigma-Aldrich, Waltham, Massachusetts, USA), 1 µL of forward primer (0.5 µM), 1 µL of reverse primer (0.5 µM), 2 µL of cDNA template, and 6 µL of nuclease-free water. Specific primers for the target gene *periostin* (forward: TAACTCCTCTATCCAGCAGA; reverse: CCACCTCCAGTAGAAATCCT) and the reference gene *GAPDH* (forward: CAAGGTCATCCATGACAACTTTG; reverse: GTCCACCACCCTGTTGCTGTAG) were used. The thermocycling protocol began with an initial denaturation at 95°C for 3 minutes, followed by 40 cycles of denaturation at 95°C for 15 seconds, and annealing/extension at 60°C for 1 minute. Gene expression levels were determined using cycle threshold (Ct) values, and data were analyzed using Eco Software v5.0 (Illumina, San Diego, California, USA). Relative expression was calculated using the $2^{-\Delta\Delta Ct}$ method using the Livak method, with results expressed as fold changes in gene expression relative to the healthy group, standardized to the *GAPDH* gene [26].

Statistical analysis

Continuous data were presented as mean and standard deviation (for normally distributed data) and median (minimum-maximum) for non-normally distributed data. Shapiro-Wilk test was utilized to assess data normality. For normally distributed data, one-way analysis of variance (ANOVA) test was conducted, while Kruskal-Wallis test was used for non-normally distributed data. Least significant difference (LSD) post-hoc test was utilized. SPSS version 26.0 software (IBM, New York, USA) was employed for data analysis, with $p<0.05$ considered statistically significant.

Results

Histopathological analysis of healthy and CRSwNP animal model

Histopathological analysis using HE staining on day 28 confirmed the successful establishment of the CRSwNP model. Six rats were excluded from the study due to mortality during the treatment period. The histological differences between the healthy and CRSwNP groups are

presented in **Figure 2**. In the healthy group, tissue sections displayed an intact epithelial architecture, consisting of simple, ciliated, goblet columnar cells (**Figure 2A**). The tubular glands were lined by columnar epithelial cells and supported by a fibrous connective tissue stroma (**Figure 2A**), which exhibited mild swelling and minimal lymphocyte infiltration (**Figure 2B**). In contrast, the CRSwNP group had typical CRSwNP pathology, with an epithelial lining ranging from simple to multilayered columnar cells, accompanied by ciliation and a thickened basement membrane (**Figure 2C**). The fibrous connective tissue stroma was markedly swollen and infiltrated with inflammatory cells, including lymphocytes, eosinophils, neutrophils, and prominent blood vessels (**Figure 2D**). These histological alterations substantiate the successful induction of CRSwNP, as reflected in the structural and cellular changes characteristic of the condition.

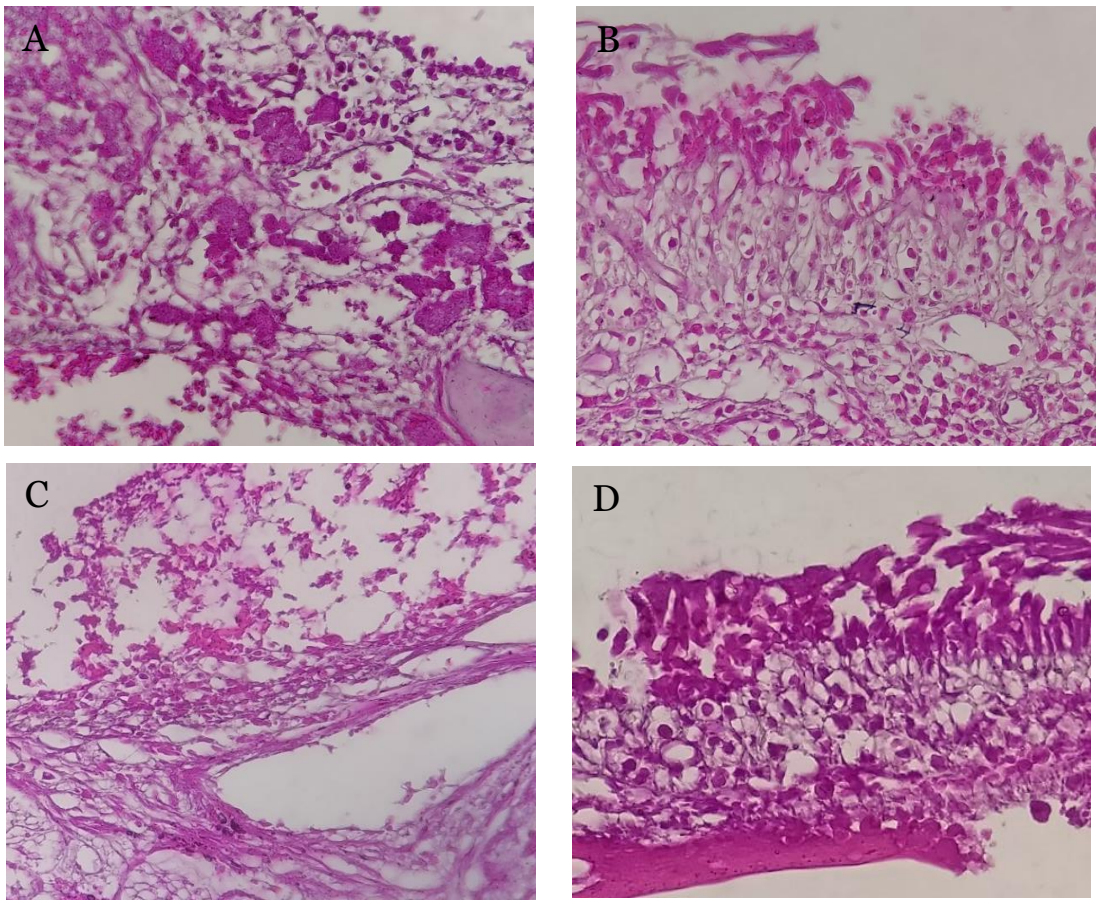

Figure 2. Histological analysis of healthy and chronic rhinosinusitis with nasal polyps (CRSwNP) groups. (A) Healthy group showed tubular glands lined by columnar epithelial cells surrounded by fibrous connective tissue. (B) Mild edema with minimal lymphocyte infiltration was observed in the healthy group. (C) CRSwNP group exhibited an epithelial lining composed of simple to multilayered columnar cells, ciliation, and a thickened basement membrane. (D) Marked edema with prominent blood vessels and infiltration by lymphocytes, eosinophils, and neutrophils was noted in CRSwNP group.

Effect of thymoquinone on p63 transcription factor expression in a CRSwNP rat model

The healthy group demonstrated sparse p63-positive areas with minimal staining intensity (**Figure 3**). In contrast, the CRSwNP group displayed the most intense brown staining, indicating the highest p63 transcription factor expression. The thymoquinone-treated group showed moderate p63 transcription factor expression, with staining intensity between that of the healthy and CRSwNP groups (**Figure 3**). One-way ANOVA revealed significantly higher p63 transcription factor expression in the CRSwNP group compared to the healthy group (p=0.001) (**Figure 3D**). Furthermore, thymoquinone treatment significantly reduced p63 transcription factor expression compared to the CRSwNP group (p<0.009). The mean percentage of p63-

positive staining was highest in the CRSwNP group (2.87±0.35%), followed by the thymoquinone-treated group (2.12±0.35%) and the healthy group (1.87±0.64%) (**Figure 3D**).

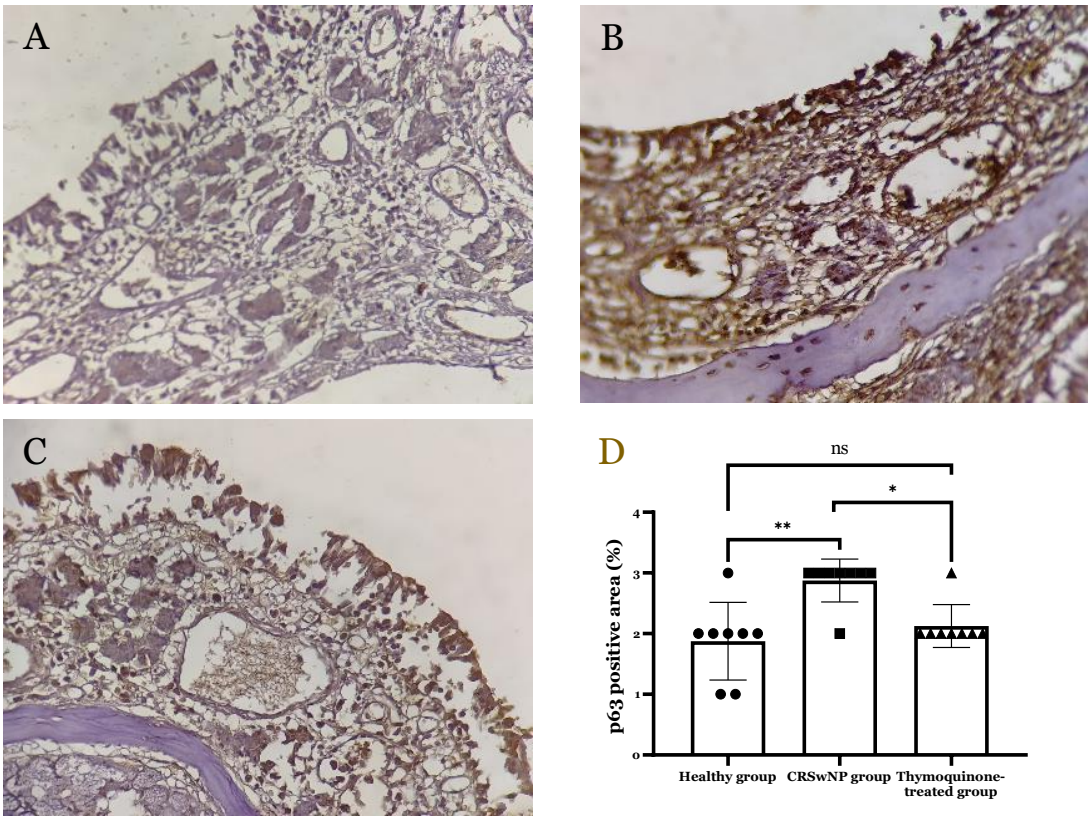

Figure 3. Effect of thymoquinone on p63 transcription factor expression in healthy group, chronic rhinosinusitis with nasal polyps (CRSwNP) group, and thymoquinone-treated group. The intensity of the brownish coloration represents positively stained epithelial cells. (A) The healthy group demonstrated sparse p63-positive areas with minimal staining intensity. (B) CRSwNP group had the most intense brown staining, indicating the highest p63 expression. (C) The thymoquinone-treated group showed moderate p63 expression, with staining intensity between that of the healthy and CRSwNP groups. (D) Effect of thymoquinone on p63 transcription factor expression in the CRSwNP rat model differed significantly among the healthy, CRSwNP, and thymoquinone-treated groups. Statistical analysis indicated a significant difference ($^{*}p<0.05$, $^{**}p<0.01$), except where noted as not significant (ns).

Effect of thymoquinone on claudin protein expression in a CRSwNP rat model

The healthy group exhibited moderate claudin protein expression, with staining intensity between that observed in the CRSwNP and thymoquinone-treated groups (**Figure 4**). The CRSwNP group displayed sparse claudin-positive areas with minimal brown staining, whereas the thymoquinone-treated group demonstrated enhanced claudin protein expression, characterized by more intense and widespread brown staining (**Figure 4**). One-way ANOVA indicated that claudin expression was lower in the CRSwNP group compared to the healthy group, although this difference was not statistically significant ($p=0.055$) (**Figure 4D**). However, the thymoquinone-treated group showed a significant increase in claudin expression compared to both the healthy and CRSwNP groups ($p=0.007$). The mean percentage of claudin-positive staining was highest in the thymoquinone-treated group (2.62±0.51%), followed by the healthy group (2.37±0.51%) and the CRSwNP group (1.62±0.74%) (**Figure 4D**).

Effect of thymoquinone on periostin mRNA expression in a CRSwNP rat model

One-way ANOVA demonstrated that periostin mRNA expression was significantly higher in the CRSwNP group compared to the healthy group ($p=0.002$) (**Figure 5**). Thymoquinone treatment significantly reduced periostin mRNA expression in the CRSwNP group ($p<0.001$), bringing levels comparable to those in the healthy group ($p=0.564$). The mean percentage of periostin

mRNA expression was highest in the CRSwNP group (17.152±9.938%), followed by the healthy group (1.000±0.000%) and the thymoquinone-treated group (0.741±0.633%).

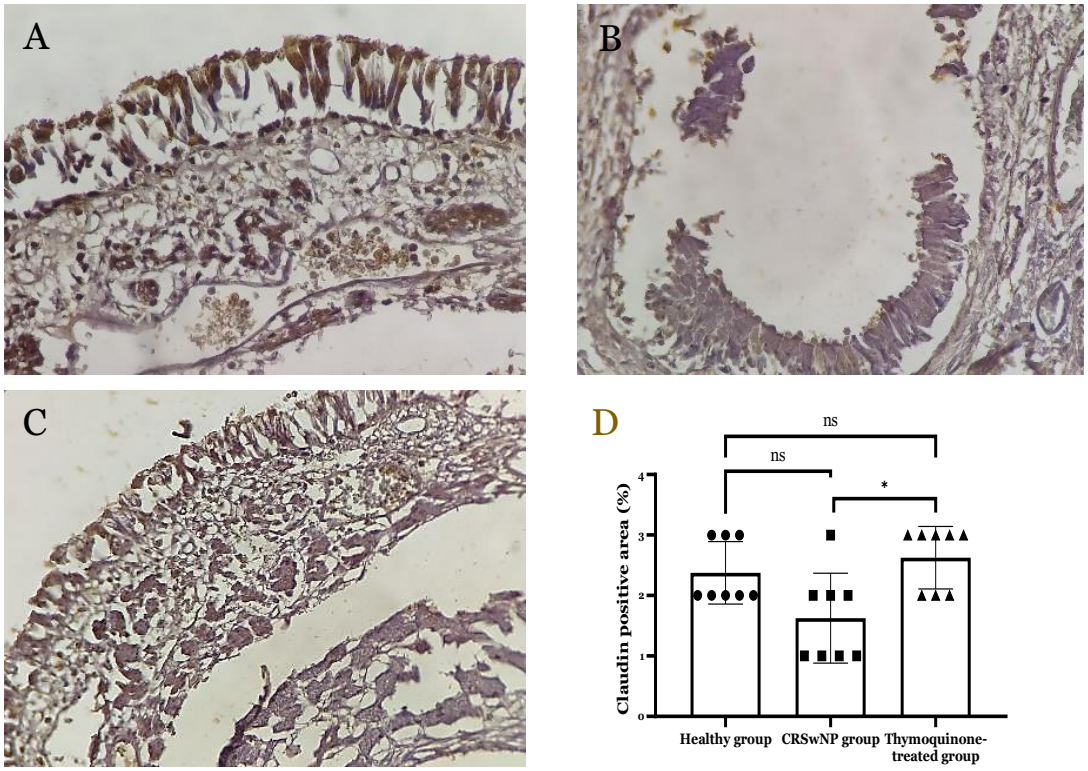

Figure 4. Effect of thymoquinone on claudin protein expression in chronic rhinosinusitis with nasal polyps (CRSwNP) rat model was assessed, which revealed varying levels of claudin-positive staining (brown) across the groups. (A) The healthy group exhibited moderate claudin expression, with staining intensity between that observed in the CRSwNP and thymoquinone-treated groups. (B) The CRSwNP group displayed sparse claudin-positive areas with minimal brown intensity. (C) The thymoquinone-treated group showed enhanced claudin expression, characterized by more intense and widespread brown coloration. (D) Effect of thymoquinone on claudin protein expression in the CRSwNP rat model revealed significant differences among the healthy, CRSwNP, and thymoquinone-treated groups. Statistical analysis indicated a significant difference ($^{*}p<0.05$), except where noted as not significant (ns).

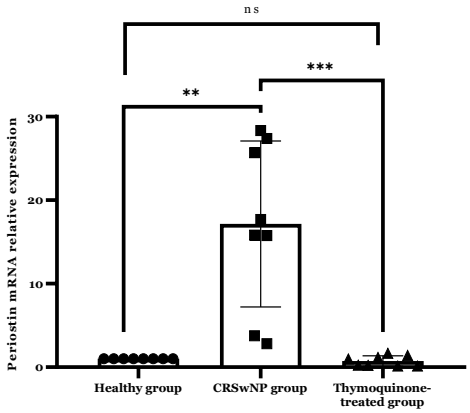

Figure 5. Effect of thymoquinone on periostin mRNA expression in the chronic rhinosinusitis with nasal polyps (CRSwNP) rat model revealed significant differences among the healthy, CRSwNP, and thymoquinone-treated groups. Statistical analysis indicated a significant difference ($^{*}p<0.05$, $^{**}p<0.01$), except where noted as not significant (ns).

Discussion

This study examined the effects of thymoquinone on the p63 transcription factor, claudin protein expression, and periostin mRNA expression in a CRSwNP animal model. Histopathological

analysis demonstrated significant epithelial and stromal changes in CRSwNP rats, including a transition of the epithelial lining from simple to multilayered columnar cells with ciliation and thickened basement membranes. The fibrous connective tissue stroma exhibited pronounced swelling, extensive inflammatory infiltration (lymphocytes, eosinophils, and neutrophils), and increased vascular prominence. These structural and cellular alterations confirm the successful establishment of the CRSwNP model, consistent with its characteristic pathological features.

This study demonstrated a significant increase in p63 transcription factor expression in CRSwNP compared to healthy rats, emphasizing its role in epithelial barrier integrity and ciliogenesis. Elevated p63 expression in the CRSwNP epithelium was associated with reduced levels of tight junction proteins, such as claudin-1 and claudin-4, highlighting its involvement in epithelial dysfunction [6]. p63, a member of the p53 family, exists in two isoforms, TAp63 and ΔNp63, and is essential for the proliferation and differentiation of epithelial basal cells [26]. Reduced p63 expression has been shown to enhance epithelial barrier function by upregulating tight junction proteins and promoting ciliogenesis in the sinonasal epithelium [15]. Tight junction proteins, including claudins, occludins, and junctional adhesion molecules, are critical for maintaining epithelial integrity [27].

Thymoquinone significantly reduces p63 transcription factor expression in a rat model of CRSwNP. Although direct evidence on the effect of thymoquinone on p63 expression in nasal polyps or CRSwNP is limited, its well-documented anti-inflammatory and immunomodulatory properties may contribute to this downregulation [27-29]. Thymoquinone has been reported to inhibit pro-inflammatory markers and signaling pathways, such as nuclear factor-kappa B (NF-κB) and transforming growth factor-beta (TGF-β), which are known to influence transcriptional regulators within the p53 family [30,31]. Additionally, thymoquinone has demonstrated the ability to mitigate epithelial damage and restore barrier function in inflammatory diseases [29], suggesting an indirect role in modulating p63 expression through the enhancement of epithelial homeostasis.

This study demonstrated that thymoquinone significantly increases claudin expression, underscoring its potential to restore tight junction protein levels in CRSwNP. Importantly, claudin expression in thymoquinone-treated CRSwNP rats showed no significant difference compared to healthy controls, indicating effective restoration of claudin expression to near-normal levels. Claudin is a vital component of tight junctions, which maintain epithelial barrier integrity in the nasal mucosa [32]. Defects in epithelial barriers are a hallmark of CRSwNP pathogenesis, characterized by significantly reduced barrier integrity compared to healthy nasal epithelium [18]. Defects in epithelial barriers are a hallmark of CRSwNP pathogenesis, characterized by significantly reduced barrier integrity compared to healthy nasal epithelium [32]. Tight junction proteins, including claudins, occludins, and junctional adhesion molecules, are critical in maintaining this integrity [5]. Furthermore, tight junction dysfunction is increasingly recognized as a contributing factor in the pathophysiology of chronic inflammatory airway diseases, such as CRS, allergic rhinitis, asthma, and chronic obstructive pulmonary disease [33].

The expression of tight junction proteins, such as claudin, is adversely affected by inflammatory mediators. Th1 cytokines (interferon-γ (IFN-γ)) and Th2 cytokines (interleukin-4 (IL-4)) have been shown to downregulate claudin expression in human sinonasal epithelial cells [4,7]. Restoration of epithelial barrier integrity has been demonstrated in a previous study, where oral corticosteroid treatment resulted in significant improvements [14]. Corticosteroids reduce the levels of inflammatory cytokines, including IFN-γ and IL-4, facilitating the restoration of tight junction protein expression [31]. Similarly, the findings of this study suggest that thymoquinone may exert a similar effect by reducing inflammation and promoting the recovery of tight junction protein expression, thereby enhancing epithelial barrier integrity in CRSwNP.

This study also demonstrated that CRSwNP significantly increases periostin mRNA expression. These findings align with a previous study that has reported periostin upregulation in CRSwNP as a key biomarker during the EMT, a process triggered by epithelial barrier disruption [34]. The EPOS 2020 guidelines recognize periostin as a critical biomarker for diagnosing CRSwNP [35]. Periostin plays a pivotal role in EMT, primarily through a TGF-β-dependent pathway [30,36]. In the pathogenesis of CRSwNP, EMT is initiated following damage

to the epithelial layer due to tight junction breakdown, which compromises the epithelial barrier [15]. This transition is characterized by the upregulation of EMT-associated markers, including extracellular matrix proteins and mesenchymal markers, with periostin being one of the most significantly increased extracellular matrix proteins [36].

Thymoquinone significantly reduced periostin expression in the CRSwNP animal model, restoring it to near-normal levels observed in the healthy group. This suggests that thymoquinone may have the potential to normalize periostin expression in CRSwNP. Although studies directly investigating thymoquinone's effect on periostin in CRSwNP are lacking, its ability to inhibit EMT markers has been demonstrated in various cancers, including bladder, breast, and gastric cancer [37,38]. Thymoquinone also suppresses goblet cell hyperplasia and inflammatory cytokines, particularly IL-4 and interleukin 13 (IL-13), which play central roles in the inflammatory cascade of CRSwNP [37,38]. Periostin interacts with integrins to mediate tissue remodeling, fibrosis, and allergic inflammation induced by Th2 cytokines, such as IL-4 and IL-13 [39]. By interacting with integrin molecules on cell surfaces, periostin further promotes EMT marker progression in epithelial cells [40]. Thymoquinone exerts its therapeutic effects by targeting these inflammatory and remodeling pathways, inhibiting goblet cell hyperplasia, reducing secretion production, and suppressing Th2 cytokines, particularly IL-4 and IL-13 [37,40]. This highlights thymoquinone's potential in mitigating periostin-associated EMT and restoring epithelial integrity in CRSwNP.

This study showed thymoquinone's therapeutic potential in restoring epithelial barrier integrity and reducing inflammatory markers in CRSwNP. Increasing claudin expression and reducing p63 and periostin levels display the potential of thymoquinone as a key to pathological features of CRSwNP, including epithelial dysfunction and EMT. These findings suggest that thymoquinone could serve as a promising alternative or aid to corticosteroids, particularly for patients with chronic inflammatory airway diseases. Furthermore, the ability of thymoquinone to modulate periostin, a biomarker recognized by the EPOS 2020 guidelines [41], highlights its relevance in clinical practice and delivers a foundation for future biomarker-targeted therapies. The broader anti-inflammatory and immunomodulatory effects of thymoquinone may also have applications in associated conditions, such as asthma and allergic rhinitis. This study primarily focused on evaluating the effects of thymoquinone on the expression of p63, claudin, and periostin genes in a rat model of CRSwNP. While the findings are promising, this study has limitations that warrant further investigation. The use of rat models may not fully replicate the complexity of the human body, necessitating validation through clinical trials. Additionally, multiple thymoquinone dosages and extending study durations should be explored to establish an effective therapeutic window and assess toxicity.

Conclusion

Thymoquinone enhances epithelial barrier integrity and reduces inflammation in a CRSwNP animal model by downregulating p63, increasing claudin expression, and suppressing periostin levels. These findings suggest its potential to restore epithelial integrity and mitigate tissue remodeling in CRSwNP, supporting further research on its efficacy and safety as a novel treatment.

Ethics approval

Ethical clearance was obtained from the Ethical Committee for Animal Research, Universitas Sumatera Utara, Medan, Indonesia (Approval number: 228/KEPK/USU/2023), and all procedures adhered to the ethical guidelines and standards of the Institutional Animal Care and Use Committee.

Acknowledgments

The authors acknowledge Mokhamad Raihan Eka Putra for assistance with language editing and valuable comments, which significantly enhanced the manuscript.

Competing interests

All the authors declare that there are no conflicts of interest.

Funding

This study received no external funding.

Underlying data

Derived data supporting the findings of this study are available from the corresponding author on request.

Declaration of artificial intelligence use

This study used artificial intelligence (AI) tools and methodologies in the following capacities of which AI-based language models ChatGPT was employed in the language refinement (improving grammar, sentence structure, and readability of the manuscript). We confirm that all AI-assisted processes were critically reviewed by the authors to ensure the integrity and reliability of the results. The final decisions and interpretations presented in this article were solely made by the authors.

How to cite

Ulfa L, Munir D, Rambe AYM, *et al*. Therapeutic potential of thymoquinone in regulating p63, claudin, and periostin in chronic rhinosinusitis with nasal polyps: An animal model study. Narra J 2025; 5 (1): e1728 - http://doi.org/10.52225/narra.v5i1.1728.

References

1. Sofyan F, Munir D, Putra IB, *et al.* Effect of thymoquinone and transforming growth factor-β1 on the cell viability of nasal polyp-derived fibroblast. Open Access Maced J Med Sci 2022;10(B):1392-1398.
2. Stevens WW, Schleimer RP, Kern RC. Chronic rhinosinusitis with nasal polyps. J Allergy Clin Immunol Pract 2016;4(4):565-572.
3. Calus L, Van Bruaene N, Bosteels C, *et al.* Twelve-year follow-up study after endoscopic sinus surgery in patients with chronic rhinosinusitis with nasal polyposis. Clin Transl Allergy 2019;9(1):30.
4. Jiao J, Wang C, Zhang L. Epithelial physical barrier defects in chronic rhinosinusitis. Expert Rev Clin Immunol 2019;15(6):679-688.
5. Schleimer RP. Immunopathogenesis of chronic rhinosinusitis and nasal polyposis. Annu Rev Pathol Mech Dis 2017;12(1):331-357.
6. Sofyan F. Efek thymoquinone terhadap viabilitas, diferensiasi, dan apoptosis sel fibroblas turunan polip hidung dengan dan tanpa pengaruh transforming growth factor-B1. Medan: Repositori Institusi Universitas Sumatera Utara; 2022.
7. Soyka MB, Wawrzyniak P, Eiwegger T, *et al.* Defective epithelial barrier in chronic rhinosinusitis: The regulation of tight junctions by IFN-γ and IL-4. J Allergy Clin Immunol 2012;130(5):1087-1096.e10.
8. Rogers GA, Den Beste K, Parkos CA, *et al.* Epithelial tight junction alterations in nasal polyposis. Int Forum Allergy Rhinol 2011;1(1):50-54.
9. Ahern S, Cervin A. Inflammation and endotyping in chronic rhinosinusitis—a paradigm shift. Medicina (Kaunas) 2019;55(4):95.
10. Kojima T, Go M, Takano K, *et al.* Regulation of tight junctions in upper airway epithelium. Biomed Res Int 2013;2013:947072.
11. Carroll DK, Brugge JS, Attardi LD. p63, cell adhesion and survival. Cell Cycle 2007;6(3):255-261.
12. Chegini Z, Didehdar M, Khoshbayan A, *et al.* The role of *Staphylococcus aureus* enterotoxin B in chronic rhinosinusitis with nasal polyposis. Cell Commun Signal 2022;20(1):29.
13. Sugita K, Kabashima K. Tight junctions in the development of asthma, chronic rhinosinusitis, atopic dermatitis, eosinophilic esophagitis, and inflammatory bowel diseases. J Leukoc Biol 2020;107(5):749-762.
14. Bequignon E, Mangin D, Bécaud J, *et al.* Pathogenesis of chronic rhinosinusitis with nasal polyps: Role of IL-6 in airway epithelial cell dysfunction. J Transl Med 2020;18(1):136.
15. Kaneko Y, Kohno T, Kakuki T, *et al.* The role of transcriptional factor p63 in regulation of epithelial barrier and ciliogenesis of human nasal epithelial cells. Sci Rep 2017;7(1):10935.
16. Mekhemar M, Hassan Y, Dörfer C. *Nigella sativa* and thymoquinone: A natural blessing for periodontal therapy. Antioxidants (Basel) 2020;9(12):1260.

17. Popa O, Băbeanu NE, Popa I, *et al.* Methods for obtaining and determination of squalene from natural sources. Biomed Res Int 2015;2015:367202.
18. Abd Al Haleem EN, Hasan WYS, Arafa HMM. Therapeutic effects of thymoquinone or capsaicin on acrylamide-induced reproductive toxicity in rats mediated by their effect on oxidative stress, inflammation, and tight junction integrity. Drug Chem Toxicol 2022;45(5):2328-2340.
19. Kojima T, Kohno T, Kubo T, *et al.* Regulation of claudin-4 via p63 in human epithelial cells. Ann N Y Acad Sci 2017;1405(1):25-31.
20. Nordin A, Kamal H, Yazid MD, *et al.* Effect of *Nigella sativa* and its bioactive compound on type 2 epithelial to mesenchymal transition: A systematic review. BMC Complement Altern Med 2019;19(1):290.
21. Tai J, Han M, Kim TH. Therapeutic strategies of biologics in chronic rhinosinusitis: Current options and future targets. Int J Mol Sci 2022;23(10):5523.
22. Treuting PM, Dintzis SM, Montine KS. Comparative anatomy and histology: A mouse, rat, and human atlas. London: Academic Press; 2017.
23. Ahn SK, Jeon SY, Khalmuratov R, *et al.* Rat model of Staphylococcal enterotoxin B-induced rhinosinusitis. Clin Exp Otorhinolaryngol 2008;1(1):24.
24. Dolci ELL, de Campos CAC, da Silva L, *et al.* Evaluation of the ability of an experimental model to induce bacterial rhinosinusitis in rabbits. Braz J Otorhinolaryngol 2014;80(6):480-489.
25. Devaraja K, Pillai S, Valiathan M, *et al.* E-cadherin expression pattern in head and neck squamous cell carcinoma and its association with clinico-pathological predictors. Egypt J Otolaryngol 2023;39(1):138.
26. Zielińska-Bliźniewska H, Paprocka-Zjawiona M, Merecz-Sadowska A, *et al.* Serum IL-5, POSTN and IL-33 levels in chronic rhinosinusitis with nasal polyposis correlate with clinical severity. BMC Immunol 2022;23(1):33.
27. Umar S, Zargan J, Umar K, *et al.* Modulation of the oxidative stress and inflammatory cytokine response by thymoquinone in the collagen induced arthritis in Wistar rats. Chem Biol Interact 2012;197(1):40-46.
28. Ahmad A, Alkharfy KM, Jan BL, *et al.* Thymoquinone treatment modulates the Nrf2/HO-1 signaling pathway and abrogates the inflammatory response in an animal model of lung fibrosis. Exp Lung Res 2020;46(3-4):53-63.
29. El Mezayen R, El Gazzar M, Nicolls MR, *et al.* Effect of thymoquinone on cyclooxygenase expression and prostaglandin production in a mouse model of allergic airway inflammation. Immunol Lett 2006;106(1):72-81.
30. Salah A, Sleem R, Abd-Elaziz A, *et al.* Regulation of NF-κB expression by thymoquinone; A role in regulating pro-inflammatory cytokines and programmed cell death in hepatic cancer cells. Asian Pac J Cancer Prev 2023;24(11):3739-3748.
31. Kurowska N, Madej M, Strzalka-Mrozik B. Thymoquinone: A promising therapeutic agent for the treatment of colorectal cancer. Curr Issues Mol Biol 2023;46(1):121-139.
32. Nur Husna SM, Tan HTT, Md Shukri N, *et al.* Nasal epithelial barrier integrity and tight junctions disruption in allergic rhinitis: Overview and pathogenic insights. Front Immunol 2021;12:663626.
33. Hellings PW, Steelant B. Epithelial barriers in allergy and asthma. J Allergy Clin Immunol 2020;145(6):1499-1509.
34. Ha JG, Cho HJ. Unraveling the role of epithelial cells in the development of chronic rhinosinusitis. Int J Mol Sci 2023;24(18):14229.
35. Balsalobre L, Pezato R, Perez-Novo C, *et al.* Epithelium and stroma from nasal polyp mucosa exhibits inverse expression of TGF-β1 as compared with healthy nasal mucosa. J Otolaryngol Head Neck Surg 2013;42(1):29.
36. Ulfa L, Munir D, Rambe M, *et al.* Histological analysis of nasal polyps in Wistar rat models. Malaysian J Med Heal Sci 2024;20:110.
37. Bantz SK, Zhu Z, Zheng T. The atopic march: Progression from atopic dermatitis to allergic rhinitis and asthma. J Clin Cell Immunol 2014;5(2):202.
38. Chiarella E, Lombardo N, Lobello N, *et al.* Nasal polyposis: Insights in epithelial-mesenchymal transition and differentiation of polyp mesenchymal stem cells. Int J Mol Sci 2020;21(18):6878.
39. Masuoka M, Shiraishi H, Ohta S, *et al.* Periostin promotes chronic allergic inflammation in response to Th2 cytokines. J Clin Invest 2012;122(7):2590-2600.
40. Malik S, Singh A, Negi P, *et al.* Thymoquinone: A small molecule from nature with high therapeutic potential. Drug Discov Today 2021;26(11):2716-2725.
41. Fokkens WJ, Lund VJ, Hopkins C, *et al.* Executive summary of EPOS 2020 including integrated care pathways. Rhinology 2020;58(2):82-111.